

Simonds, *J. Biol. Chem.* **271**, 20208 (1996); K. Blüml et al., *EMBO J.* **16**, 4908 (1997); J. Yamauchi, Y. Kaziro, H. Itoh, *J. Biol. Chem.* **272**, 7602 (1997).
 26. J. Sondel, A. Bohm, D. G. Lambright, H. E. Hamm, P. B. Sigler, *Nature* **379**, 369 (1996).
 27. Recombinant baculovirus containing bovine H₆Gy2 cDNA was provided by A. Gilman (University of Texas Southwestern Medical Center, Dallas, TX). The H₆-Q227L-Gs α was from T. Patel (University of Tennessee, Memphis). The baculovirus vector encoding human PLC- β 2 modified with an NH₂-terminal H₆ tag was pro-

vided by A. Smrcka (University of Rochester, NY). We thank K. Schey (Medical University of South Carolina, Charleston) for performing the mass spectrometry analysis on the recombinant G β γ proteins.

28. Supported as follows: Ford Foundation Fellowship (C.E.F.), American Heart Association Grant-in-Aid (N.P.S.), Aaron Diamond Fellowship (G.W.), and both the Mella and Leon Benziyo Center for Neuroscience and Behavioral Research and the Joseph Cohn Center for Biomembrane Research (E.R.). USPHS grants DA02575, DA02121, MH40165,

NS33502, DK42086, and DK44840 (R.J.M.); DK38761 and GM54508 (R.L.); and EY06062 and EY10291 (H.E.H.); Howard Hughes Medical Institute (L.Y.J. and R.J.L.), a National Institutes of Mental Health grant to the Silvio Conte Center for Neuroscience at UCSF (L.Y.J.), and both a Distinguished Investigator Award from the National Association for Research in Schizophrenia and Depression and an American Heart Association Grant-in-Aid (H.E.H.).

26 February 1998; accepted 25 March 1998

Distinct WNT Pathways Regulating AER Formation and Dorsoventral Polarity in the Chick Limb Bud

Mineko Kengaku,*† Javier Capdevila,*
 Concepción Rodríguez-Esteban,* Jennifer De La Peña,
 Randy L. Johnson, Juan Carlos Izpisua Belmonte,‡§
 Clifford J. Tabin§

The apical ectodermal ridge (AER) is an essential structure for vertebrate limb development. *Wnt3a* is expressed during the induction of the chick AER, and misexpression of *Wnt3a* induces ectopic expression of AER-specific genes in the limb ectoderm. The genes β -catenin and *Lef1* can mimic the effect of *Wnt3a*, and blocking the intrinsic *Lef1* activity disrupts AER formation. Hence, *Wnt3a* functions in AER formation through the β -catenin/LEF1 pathway. In contrast, neither β -catenin nor *Lef1* affects the *Wnt7a*-regulated dorsoventral polarity of the limb. Thus, two related *Wnt* genes elicit distinct responses in the same tissues by using different intracellular pathways.

The *Wnt* gene family encodes a group of signaling molecules that are implicated in numerous aspects of morphogenesis in both vertebrates and invertebrates. Several chick *Wnt* genes are expressed in a specialized epithelial structure running along the distal margin of the limb bud, called the apical ectodermal ridge (AER), which is essential for limb morphogenesis (1, 2). *Wnt3a* is the first of these genes to be expressed in the limb. We therefore examined the spatio-temporal pattern of expression of *Wnt3a* in developing limb buds with respect to that of *Fgf8*, the earliest known AER marker during chick development (3, 4) (Fig. 1, A through D) (5).

Wnt3a transcripts are detected before

Fgf8 transcripts in the limb field ectoderm but not in the flank outside the limb fields. Subsequently, *Wnt3a* expression is up-regulated in the ectoderm cells near the dorsoventral (DV) border. *Fgf8* expression is initiated and then up-regulated within the region of high *Wnt3a* expression during AER formation. From stage 20 on, *Wnt3a* and *Fgf8* expression are confined primarily to the mature AER. Thus, *Wnt3a* expression appears to presage *Fgf8* expression and AER formation.

To verify the epistatic relationship between *Wnt3a* and *Fgf8* that is suggested by the expression data, we ectopically delivered each factor to developing limb buds. We misexpressed *Wnt3a* in the limb ectoderm using a replication-competent retroviral vector and assayed for the expression patterns of the various AER markers (6). Misexpression of *Wnt3a* induced ectopic expression of AER-specific genes, including *Bmp2*, *Fgf4*, and *Fgf8*, in broad patchy domains in the ectoderm of nearly 100% of infected limbs (Fig. 1E) (5). However, *Wnt3a* expression was not induced in the ectoderm by either fibroblast growth factor 4 (FGF4) protein or *Fgf8*-virus (5). This suggests that *Wnt3a* acts upstream of FGFs in establishing AER gene expression.

In addition to its effect on AER gene expression, *Wnt3a* misexpression occasion-

ally led to disruption of the AER or to formation of an ectopic AER extending ventrally, or both (Fig. 1, E and F). These morphological effects on the AER are reminiscent of those seen after misexpression of *Radical fringe* (7). We therefore examined *Radical fringe* expression and found that it was ectopically expressed in *Wnt3a*-infected limbs (8). Disruption of the AER morphology was only seen in a subset of *Wnt3a*-infected limb buds, which is consistent with the finding that *Radical fringe* only affects AER formation when it is misexpressed at the earliest stages of limb development (7).

The FGFs produced in the AER are responsible for maintaining the proliferative state of the undifferentiated mesoderm at the distal tip of the limb bud, the progress zone (PZ) (1). To verify that the FGFs induced in the limb bud ectoderm by *Wnt3a* are functional signals, we examined the expression of several PZ markers: *Fgf10* (9), *Msx1* (10), *Nmyc* (11), and *Slug* (12). Equivalent results were obtained with each of these markers (Fig. 2) (8). When the AERs were removed from experimental limb buds, expression of the PZ markers was rapidly lost (Fig. 2, C and D). Application of *Wnt3a*-expressing cells to the AER-deprived limbs induced *Fgf8* expression and restored expression of the PZ markers (Fig. 2, E and F). To show that this response was due to the ectopic expression of FGFs and not to a direct action of *Wnt3a* itself, we removed the adjacent distal ectoderm as well as the AER so that the *Wnt3a* cells could not induce ectodermal *Fgf8* expression (Fig. 2G). Under these conditions, *Wnt3a* induced little or no expression of the PZ genes (Fig. 2H). The maintenance of the PZ is critical for outgrowth of the limb bud. The long-term effects of virally mediated *Wnt3a* misexpression, and consequent ectopic FGF production by the ectoderm, included some cases in which extra outgrowth formed digitlike structures (5). *Wnt3a* thus appears to influence both morphological AER formation and induction of AER-specific genes in the early limb bud.

The members of the vertebrate *Wnt* gene family have been categorized by their relative ability to transform murine mammary epithelial cells (13). A similar classification can be made on the basis of the ability to

M. Kengaku and C. J. Tabin, Department of Genetics, Harvard Medical School, 200 Longwood Avenue, Boston, MA 02115, USA.

J. Capdevila, C. Rodríguez-Esteban, J. De La Peña, J. C. I. Belmonte, The Salk Institute for Biological Studies, 10010 North Torrey Pines Road, La Jolla, CA 92037, USA.

R. L. Johnson, Department of Biochemistry and Molecular Biology, M.D. Anderson Cancer Center, University of Texas, 1515 Holcombe Boulevard, Houston, TX 77030, USA.

*These authors contributed equally to this work.

†Present address: Department of Biophysics, Kyoto University, Sakyo-ku, Kyoto 606, Japan.

‡To whom correspondence should be addressed. E-mail: belmonte@salk.edu

§The laboratories of these authors contributed equally to this study.

promote axis duplications in early *Xenopus* embryos (14). Yet even *Wnt* genes categorized into the same functional group can play distinct roles during limb development. During the period of AER formation, *Wnt7a*, which is placed in the same highly transforming axis-duplicating class as *Wnt3a*, is exclusively expressed in the dorsal limb ectoderm (15, 16) and functions as the signal for DV patterning in the distal limb (17–19). In early stages of limb development, expression domains of *Wnt3a* and *Wnt7a* overlap in the dorsal ectoderm. To assess whether the two *Wnt* family genes are functionally redundant, we compared their abilities to induce expression of AER markers and affect DV patterning. Early limb buds were infected with either *Wnt3a* or *Wnt7a* virus (5) and examined for *Fgf8* expression (Fig. 3, A, C, and E). Unlike misexpression of *Wnt3a*, misexpression of *Wnt7a* never affected the expression pattern of *Fgf8* or the morphology of the AER, which suggests that *Wnt7a* is not involved in AER formation. The effects of *Wnt3a* and *Wnt7a* on DV patterning were assayed by monitoring expression of the dorsal mesenchymal marker *Lmx1* (Fig. 3B). Misexpression of *Wnt7a* induced strong ectopic expression of *Lmx1* in the distal half of ventral mesenchyme (Fig. 3F), and produced a biconvex-shaped limb bud, in contrast to the normal ventrally curving limb bud morphology (Fig. 3, B and F) (17, 18). *Wnt3a* misexpression did not produce the morphological bidorsal phenotype and had little or no effect on *Lmx1* expression (Fig. 3D).

To understand how these two *Wnt* genes elicit distinct responses, we investigated whether *Wnt3a* and *Wnt7a* act through the same signaling pathway. In other systems, signaling by the highly transforming *Wnt* genes, including *Wnt3a*, has been shown to be transduced by preventing degradation of cytoplasmic β -catenin, a protein that is ubiquitously expressed in vertebrate embryos (20–22). We misexpressed an activated mutant form of β -catenin (20, 23, 24) in limb buds (5) and found that β -catenin activity simulated the effect of *Wnt3a* but not of *Wnt7a*. Misexpression of the activated form of β -catenin induced ectopic expression of *Fgf8* (Fig. 3G) and expression of other AER markers, including *Fgf4* and *Bmp2*, in the ectoderm and up-regulated the downstream PZ markers *Msx1* and *Nmyc* in the mesoderm (8). In contrast, misexpression of β -catenin did not induce the strong mesenchymal expression of *Lmx1* seen in response to *Wnt7a* (Fig. 3H). Moreover, like *Wnt3a*-infected limb buds, activated β -catenin-infected limbs retain a concave ventral morphology in contrast to the biconvex morphology of *Wnt7a*-infected ones

(Fig. 3, D, F, and H). Thus, *Wnt3a* and *Wnt7a* function in limb morphogenesis through β -catenin-dependent and -independent pathways, respectively.

β -catenin forms a complex with members of the LEF/XTCF family to activate

Fig. 1. *Wnt3a* induces AER gene expression and regulates AER formation. (A through D) Spatiotemporal relationship between *Wnt3a* and *Fgf8* expression during early limb development. Images are of whole-mount in situ hybridization showing expression patterns of *Wnt3a* [(A) and (B)] and *Fgf8* [(C) and (D)]. At stage 15, *Wnt3a* expression is detected in the surface ectoderm overlying the lateral plate mesoderm at approximately the level of somites 14 to 18 [between arrowheads in (A)], whereas *Fgf8* expression is not detected in the limb field [between arrowheads in (C)] before stage 16 (5). As the limb buds emerge, expression of *Wnt3a* becomes elevated in the distal limb ectoderm forming the AER, whereas it is maintained at a lower level in the proximal dorsal ectoderm of the limb (8). Once the AER has formed, both *Wnt3a* (B) and *Fgf8* (D) are primarily confined to the AER through at least stage 26. (E and F) Misexpression of *Wnt3a* induces ectopic expression of an AER-specific gene, *Fgf8*, in patches on both the dorsal and ventral ectoderm. Occasionally there are also morphological effects on the AER. In some cases, the AER appears wider in places, giving it an irregular appearance [green arrowhead in (E)]. In other cases, the AER is disrupted [red arrowhead in (F)] or ectopic AERs form, branching toward the ventral side [yellow arrowhead in (F)]. Panels show lateral views of the limbs, dorsal side up. Single- and double-color whole-mount in situ hybridizations of chick embryos were performed as described (36). The probes used were *Wnt3a* [372 base pairs (bp) (32)] and *Fgf8* [800 bp (4)].

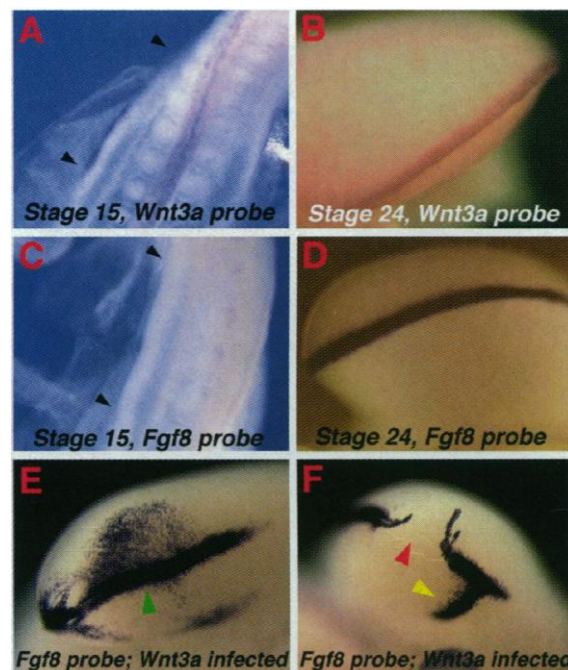
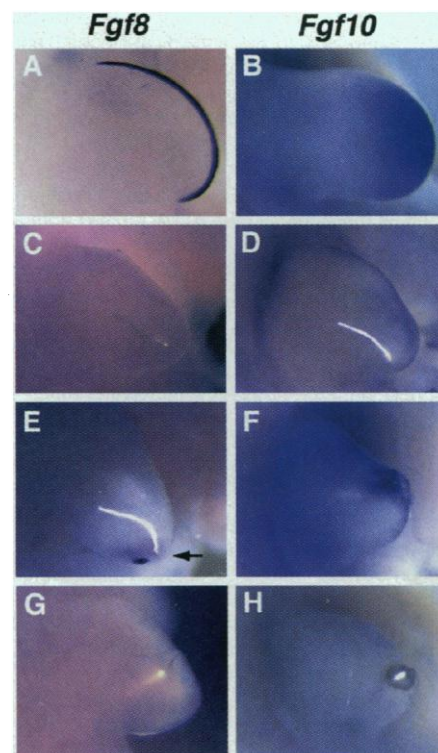


Fig. 2. Induction of PZ gene expression by *Wnt3a* requires the ectoderm expressing *Fgf8*. Embryos were manipulated at stage 20 and harvested after 24 hours for in situ hybridization for *Fgf8* [(A), (C), (E), and (G)] and *Fgf10* (probed with a 555-bp fragment; a gift from H. Ohuchi) [(B), (D), (F), and (H)]. (A and B) Normal expression patterns in the contralateral limbs. *Fgf8* (A) is specifically expressed in the AER, whereas *Fgf10* (B) is strongly expressed in the PZ. (C and D) The AERs were removed with fine tungsten needles and forceps and replaced with control line 0 cell pellets fixed with a platinum staple at the distal rim of the mesoderm. In the absence of the AER, there is no expression of *Fgf8* (C) or of other members of the *Fgf* family, and expression of *Fgf10* disappears within 20 hours (D). (E and F) The AERs were removed and replaced with *Wnt3a* cell pellets. (E) *Wnt3a* induces *Fgf8* expression (purple staining) in the ectoderm adjacent to implanted cell pellets expressing *Wnt3a* (pink staining pointed to by an arrow, reflecting a second hybridization with a 900-bp probe detecting the viral vector). (F) Expression of *Fgf10* is restored in the distal mesenchyme next to *Wnt3a* cell pellets. (G and H) The limb buds were denuded of the distal ectoderm on both the dorsal and the ventral sides as well as the AERs, and then *Wnt3a* cell pellets were implanted. The proximal ectoderm was left intact. *Wnt3a* cell pellets induced neither *Fgf8* (G) nor *Fgf10* expression (H).



transcription of downstream genes (25–28). To explore the possible involvement of LEF1 in WNT3a signaling, we cloned a chick

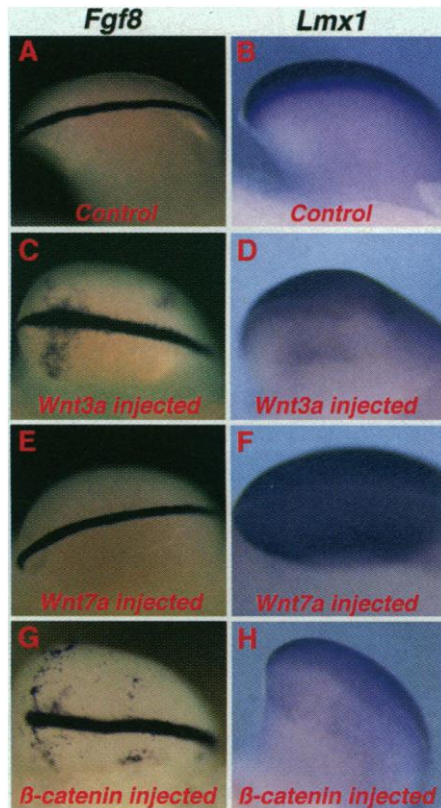


Fig. 3. WNT3a and WNT7a elicit distinct activities that are differentially mediated by β -catenin. Embryos were infected with virus carrying *Wnt3a* [(C) and (D)], *Wnt7a* (16) [(E) and (F)], or an activated form of β -catenin (5) [(G) and (H)] at stage 10 and harvested at stage 24 to analyze expression of *Fgf8* [(A), (C), (E) and (G)] and *Lmx1* [(B), (D), (F), and (H)]. The different viruses all resulted in comparable infections, spread throughout the limb ectoderm and mesoderm (5). Ectodermal targets are, in general, induced in a patchy pattern, whereas mesodermal targets are more uniformly induced, perhaps reflecting the relative kinetics of viral spread in the two tissues. (A and B) Normal expression of *Fgf8* and *Lmx1*. *Fgf8* expression is ectopically induced in the limb ectoderm by *Wnt3a* (C) in nearly 100% of infections, but never by *Wnt7a* (E). In contrast, *Lmx1* expression is strongly induced throughout the ventral mesenchyme by *Wnt7a* in nearly 100% of infections (F) but not by *Wnt3a* (D). (D) In 20 to 30% of infected limbs, *Wnt3a* induces patchy weak expression in the ventral mesenchyme and shifts the distal border of *Lmx1* expression slightly ventral to the AER (5), which appeared to be correlated with the formation of widened and ectopic AERs. Activated β -catenin is able to mimic *Wnt3a* in inducing ectopic *Fgf8* expression in the dorsal and the ventral ectoderm (G) and both the punctate ventral expression and the ventral shift in the distal border of *Lmx1* expression (H) (5) at a comparable frequency. However, activated β -catenin does not induce strong ventral expression of the *Wnt7a* target *Lmx1* in the mesenchyme.

homolog of *Lef1*. *Lef1* is strongly expressed in the AER and distal mesenchyme of the chick limb primordia (Fig. 4A). In addition to the limb buds, intense expression is observed in the developing medial somites and in the tail bud (8), both of which are regions believed to be targets of *Wnt3a* signaling (29, 30).

To examine whether *Wnt3a* regulates *Lef1* expression during chick development, embryos were injected with *Wnt3a* virus at stage 10 and assayed for *Lef1* expression at stages 22 to 24. Misexpression of *Wnt3a* markedly enhanced *Lef1* expression in both the ectoderm and mesoderm of the limb bud and also in the tail bud (Fig. 4B) (8). Misexpression of *Wnt7a* had no effect on *Lef1* expression (Fig. 4C). Thus, *Lef1* is a specific target of WNT3a signaling.

To test whether the up-regulation of *Lef1* mediates the WNT3a effects on AER marker genes, we misexpressed a retrovirus carrying *Lef1* in the ectoderm of developing limb buds. *Fgf8* expression was ectopically induced in the infected limb ectoderm (Fig. 4D). However, like *Wnt3a* and β -catenin, *Lef1* was unable to mimic the ability of *Wnt7a* to induce *Lmx1* expression (8).

To assess whether LEF1 activity is necessary for the induction of AER morphogenesis by WNT3a, we constructed a retrovirus carrying a deleted form of *Lef1* cDNA (Δ *Lef1*) that binds to DNA but not to

β -catenin, thereby blocking intrinsic *Lef1* activity as a dominant negative mutant (27, 28). Misexpression of Δ *Lef1* disrupted the AER and subsequently perturbed normal growth of the underlying mesenchyme, resulting in severe defects in limb outgrowth and patterning (Fig. 4E). However, expression of the WNT7a target *Lmx1* was not suppressed by misexpression of Δ *Lef1* (Fig. 4F). Thus the β -catenin/LEF1 pathway is necessary and sufficient to induce a WNT3a response but not a WNT7a response.

Apparently, *Lef1* is both a target and a mediator of WNT3a signaling. In the early *Xenopus* embryo, the preexisting level of the *Lef1* homolog XTCTF3 is effectively saturating (25, 27). In contrast, we find that in the chick limb bud, increased expression of LEF1 activates *Wnt3a* targets. Obviously, ectodermal cells must be capable of responding to WNT3a before LEF1 up-regulation. This could be mediated by the low preexisting levels of LEF1, which we observe throughout the ectoderm, in which case the LEF1 induction would constitute a positively reinforcing feedback loop. Alternatively, the induction of *Lef1* could be supported by another member of the LEF1 family (31).

Our results suggest that WNT3A/ β -catenin/LEF1 signaling plays a key role in endogenous chick AER formation. Surpris-

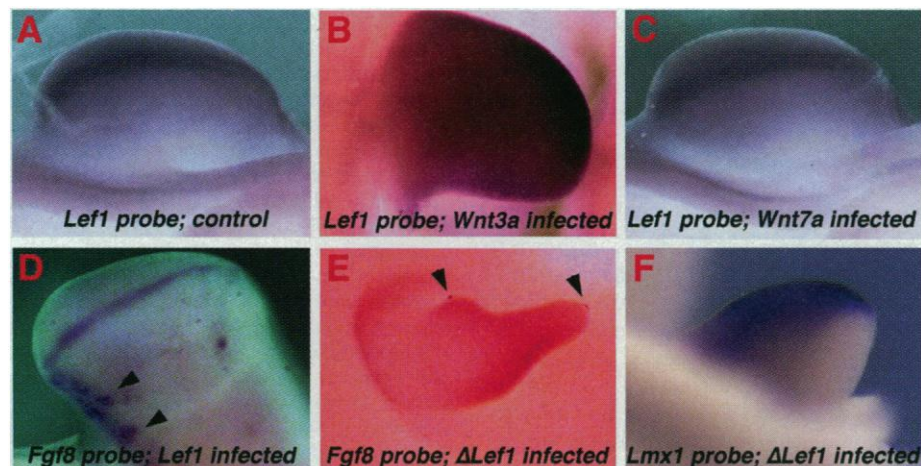


Fig. 4. LEF1 mediates signaling by WNT3a but not WNT7a. (A) Expression of chick *Lef1* in a stage-23 limb bud. (B and C) *Lef1* expression is enhanced and ectopically induced in the entire limb bud by *Wnt3a* misexpression [(B), dorsal view] but not by *Wnt7a* misexpression (C). (D) Misexpression of *Lef1* in the limb bud induces ectopic expression of *Fgf8* (arrowheads). (E) Blocking *Lef1* activity by Δ *Lef1* misexpression suppresses *Fgf8* expression in the AER and disrupts formation of the morphological AER. Gaps in *Fgf8* expression (between arrowheads) are seen where the morphological AER is disrupted. Limb outgrowth at the gaps is markedly retarded. (F) Expression of *Lmx1* in the dorsal mesenchyme is not suppressed by misexpression of Δ *Lef1* in the infected limb, which is reduced in size because of disruption of the AER. The full-length chick *Lef1* gene was cloned by screening a cDNA library of a chick limb bud at stage 20 to 22 under reduced stringency conditions by hybridization with an approximately 1.0-kb *Lef1* mouse cDNA. The full-length sequence has been deposited in the GenBank database under accession number A-F 064462. The entire coding frame of chick *Lef1* and the deletion mutant of chick *Lef1* deprived of 31 NH₂-terminal amino acids (Δ *Lef1*) were cloned into RCAS(BP)A as described in (6).

ingly, *Wnt3a* is neither expressed in the AER nor implicated in its formation during mouse limb development (15, 30). Several other *Wnt* genes have also been shown to be expressed differentially between mouse and chick embryos, both in the developing central nervous system and in limb buds, including some in the murine AER (15, 32). Different *Wnt* genes could substitute for one another as long as they activate the same intracellular signaling pathway mediated by β -catenin/LEF1. It is therefore probable that another species of *Wnt* that is expressed in the mouse AER plays the same role as *Wnt3a* in the chick.

Both WNT3a and WNT7a proteins act, at least in part, on the mesoderm, where they activate distinct targets; WNT3a induces *Lef1* whereas WNT7a induces *Lmx1*, which implies that receptors for both factors must be present on the surface of mesenchymal cells. In spite of previous data suggesting that all members of the highly transforming class of *Wnt* genes act through β -catenin, our results indicate that the induction of *Lmx1* expression by WNT7a signaling is not mediated by β -catenin and LEF1. Precedent exists for more divergent *Wnt* genes, such as *Wnt5a*, to act through distinct signaling cascades (33). Transcriptional activation of downstream genes by distinct WNT pathways allows for their different inductive roles in the same tissue during development.

REFERENCES AND NOTES

1. R. L. Johnson and C. L. Tabin, *Cell* **90**, 979 (1997).
2. M. Kengaku, V. Twombly, C. Tabin, *Cold Spring Harbor Symp. Quant. Biol.* **L12**, 421 (1998); Y. Yang and A. McMahon, personal communication.
3. A. Vogel, C. Rodriguez, J. C. Izpisua-Belmonte, *Development* **122**, 1737 (1996).
4. P. H. Crossley, G. Minowada, C. A. MacArthur, G. R. Martin, *Cell* **84**, 127 (1996).
5. See supplementary figures at www.sciencemag.org/feature/data/976400.shl.
6. A mouse *Wnt3a* cDNA encoding the entire open reading frame and a deleted mutant of β -catenin containing the internal *Armadillo* repeats that acts as a stable constitutively activated variant (23) were individually cloned into the shuttle vector SLAX-13 and then subcloned into retroviral vector RCAS(BP)A (34). Retrovirus was produced using a line 0 chick embryo fibroblast and harvested as described (35). Embryos at stage 9 to 11 were injected in the fore- or hindlimb primordia. This protocol results in widespread infection of the limb ectoderm by the time the embryos are harvested at stage 22 to 24 for whole-mount in situ hybridization (7, 8, 17). A significant number of samples (>10) were analyzed in each case. To generate embryos primarily infected in the limb ectoderm, injection was targeted onto the external surface of the ectoderm underneath the vitelline membrane.
7. E. Laufer *et al.*, *Nature* **386**, 366 (1997); C. Rodriguez-Esteban *et al.*, *ibid.*, p. 360.
8. M. Kengaku *et al.*, unpublished data.
9. H. Ohuchi *et al.*, *Development* **124**, 2235 (1997).
10. Y. Yokouchi, K. Ohsugi, H. Sasaki, A. Kuroiwa, *ibid.* **113**, 431 (1991); M. A. Ros *et al.*, *ibid.* **116**, 811 (1992).
11. S. Sawai, K. Kato, Y. Wakamatsu, H. Kondoh, *Mol. Cell. Biol.* **10**, 2017 (1990).

12. M. A. Ros, M. Sefton, M. A. Nieto, *Development* **124**, 1821 (1997).
13. G. T. Wong, B. J. Gavin, A. P. McMahon, *Mol. Cell. Biol.* **14**, 6278 (1994).
14. S. J. Du, S. M. Purcell, J. L. Christian, L. L. McGrew, R. T. Moon, *ibid.* **15**, 2625 (1995); R. T. Moon, J. D. Brown, M. Torres, *Trends Genet.* **13**, 157 (1997).
15. B. A. Parr, M. J. Shea, G. Vassileva, A. P. McMahon, *Development* **119**, 247 (1993).
16. B. J. Gavin, J. A. McMahon, A. P. McMahon, *Genes Dev.* **4**, 2319 (1990); C. N. Dealy, A. Roth, D. Ferrari, A. M. Brown, R. A. Koshier, *Mech. Dev.* **43**, 175 (1993).
17. R. D. Riddle *et al.*, *Cell* **83**, 631 (1995).
18. A. Vogel, C. Rodriguez, W. Warnken, J. C. Izpisua Belmonte, *Nature* **378**, 716 (1995).
19. P. A. Parr and A. P. McMahon, *ibid.* **374**, 350 (1995).
20. C. Yost *et al.*, *Genes Dev.* **10**, 1443 (1996); B. Rubinfeld *et al.*, *Science* **275**, 1790 (1997).
21. J. R. Miller and R. T. Moon, *Genes Dev.* **10**, 2527 (1996).
22. L. L. McGrew, C. J. Lai, R. T. Moon, *Dev. Biol.* **172**, 337 (1995).
23. N. Funayama, F. Fagotto, P. McCreary, B. M. Gumbiner, *J. Cell Biol.* **128**, 959 (1995).
24. P. J. Morin *et al.*, *Science* **275**, 1787 (1997).
25. J. Behrens *et al.*, *Nature* **382**, 638 (1996); O. Huber *et al.*, *Mech. Dev.* **59**, 3 (1996).
26. E. Brunner, O. Peter, L. Schweizer, K. Basler, *Nature* **385**, 829 (1997); J. Riese *et al.*, *Cell* **88**, 777 (1997).
27. M. Molenaar *et al.*, *Cell* **86**, 391 (1996).
28. M. van de Wetering *et al.*, *ibid.* **88**, 789 (1997).

29. A. E. Munsterberg, J. Kitajewski, D. A. Bumcrot, A. P. McMahon, A. B. Lassar, *Genes Dev.* **9**, 2911 (1995); M. Maroto *et al.*, *Cell* **89**, 139 (1997); T. L. Greco *et al.*, *Genes Dev.* **10**, 313 (1996).
30. S. Takada *et al.*, *Genes Dev.* **8**, 174 (1994).
31. S. Noramly, J. Pisenati, U. Abbott, B. Morgan, *Dev. Biol.* **179**, 339 (1996); J. Gastrop, R. Hoevenagel, J. R. Young, H. C. Clevers, *Eur. J. Immunol.* **22**, 1327 (1992).
32. M. Hollyday, J. A. McMahon, A. P. McMahon, *Mech. Dev.* **52**, 9 (1995).
33. D. C. Slusarski, J. Yang-Snyder, W. B. Busa, R. T. Moon, *Dev. Biol.* **182**, 114 (1997); D. C. Slusarski, V. G. Corces, R. T. Moon, *Nature* **390**, 410 (1997).
34. S. H. Hughes, J. J. Greenhouse, C. J. Petropoulos, P. Suttrave, *J. Virol.* **61**, 3004 (1987).
35. B. A. Morgan and D. M. Fekete, *Methods Cell Biol.* **51**, 185 (1996).
36. M. Levin, R. L. Johnson, C. D. Stern, M. Kuehn, C. Tabin, *Cell* **82**, 803 (1995); R. D. Riddle, R. L. Johnson, E. Laufer, C. Tabin, *ibid.* **75**, 1401 (1993).
37. We thank A. McMahon and Y. Yang for sharing data before publication and providing the chick *Wnt3a* probe and the mouse *Wnt3a* cDNA, and B. Eshelman for technical expertise. This work was supported by a grant from the American Cancer Society to C.J.T., grants from NIH and the G. Harold and Leyla Mathers Charitable Foundation to J.C.I.B., a fellowship from the Japan Society for the Promotion of Science to M.K., and a fellowship from the Fulbright/Spanish Ministry of Education to J.C.

26 November 1997; accepted 21 April 1998

X-ray Crystal Structure of C3d: A C3 Fragment and Ligand for Complement Receptor 2

Bhushan Nagar,* Russell G. Jones,* Russell J. Diefenbach,† David E. Isenman, James M. Rini‡

Activation and covalent attachment of complement component C3 to pathogens is the key step in complement-mediated host defense. Additionally, the antigen-bound C3d fragment interacts with complement receptor 2 (CR2; also known as CD21) on B cells and thereby contributes to the initiation of an acquired humoral response. The x-ray crystal structure of human C3d solved at 2.0 angstroms resolution reveals an α - α barrel with the residues responsible for thioester formation and covalent attachment at one end and an acidic pocket at the other. The structure supports a model whereby the transition of native C3 to its functionally active state involves the disruption of a complementary domain interface and provides insight into the basis for the interaction between C3d and CR2.

Serum complement protein C3 is a central component of host defense because its proteolytic activation is the point of convergence of the classical, alternative, and lectin pathways of complement activation. C3 cleavage products mediate many of the effector functions of humoral immunity, including inflammation, opsonization, and

cytolysis. Proteolytic cleavage of C3 into C3a and C3b exposes an internal thioester bond that through transacylation mediates covalent attachment of C3b to the surface of foreign pathogens (1). Although surface-bound C3b is itself a ligand for complement receptor 1 (CR1; also known as CD35), it can subsequently be degraded into the successively smaller fragments iC3b and C3dg, tagging the pathogen for recognition by other receptors, including the B cell complement receptor CR2 (CD21) (1). The interaction between B cell CR2 and antigen-bound iC3b or C3dg is an essential component of a normal antibody response (2), making an important link between the innate and adaptive arms of the immune system (3). The C3d fragment (a CR2-

Department of Biochemistry and Department of Molecular and Medical Genetics, University of Toronto, Toronto, Ontario, M5S 1A8, Canada.

*These authors contributed equally to this work.
 †Present address: Centre for Virus Research, Westmead Hospital, University of Sydney, Westmead, NSW 2145; Australia.
 ‡To whom correspondence should be addressed at the Department of Molecular and Medical Genetics, University of Toronto, Toronto, Ontario, Canada, M5S 1A8. E-mail: james.rini@utoronto.ca